

# **Experimental Investigation of Smoothing by Spectral Dispersion with Apertured Near Fields**

Ming-fai Fong

Summer High School Student Program 2000  
LABORATORY FOR LASER ENERGETICS  
University of Rochester  
250 East River Road  
Roschester, NY 14623-1299

## **Abstract**

Far field intensity distributions of an OMEGA laser beam were measured with apertured near fields. A rectangular slit of width one sixth the near field diameter was placed in the near field and the orientation of the slit was aligned along each of the two SSD axes. Power spectra of measured far fields were computed for the two slit orientations. One nanosecond square laser pulses smoothed with 1 THz SSD and distributed polarization rotators were studied. Simulations show good agreement with the experimental data. This investigation can be extrapolated to SSD smoothing of beams that irradiate only a portion of the phase plate, such as the ultrafast picket fence pulse.

## INTRODUCTION

Laser beam smoothing is essential for direct-drive inertial confinement fusion.[1] Nonuniformities in laser-irradiation imprint target mass perturbations, which seed the ablative Rayleigh-Taylor hydrodynamic instability and degrade target performance. Laser-irradiation nonuniformities are reduced using the following smoothing techniques: (1) smoothing by spectral dispersion (SSD), (2) distributed phase plates (DPPs), and (3) distributed polarization rotators (DPRs). In this research far field intensity distributions of an OMEGA laser beam were measured with apertured near fields. A rectangular slit of width one-sixth the near field diameter was placed in the near field and the orientation of the slit was aligned along each of the two SSD axes. Power spectra of measured far fields were computed for the two slit orientations. One-nanosecond square laser pulses smoothed with 1 THz SSD and distributed polarization rotators were studied.

The following sections discuss (1) a brief background of Fourier analysis, (2) the experimental set up of the investigation, (3) the technique used to align the rectangular slit along either of the two SSD bandwidth axes, (4) the analysis of far field measurements of pulses with 1 THz SSD and DPRs, and (5) the calculated power spectral densities of these pulses in comparison with theoretical predictions. This investigation shows that the simulations for SSD smoothing of beams with apertured near fields are in good agreement with the experimental results. It can also be extrapolated to SSD smoothing of beams that irradiate only a portion of the phase plate, such as the ultrafast picket fence pulse.[2]

## FOURIER ANALYSIS

Fourier analysis was essential in this research. Initially the far field intensity of a near field with a rectangular aperture and no laser beam smoothing was modeled. Fig. 1a shows the near field intensity (the square of the electric field). The apertured beam cross-section has -

constant intensity. The far field image, shown in Fig. 1b, is created by taking a 2-D Fourier transform of the near field electric field. The speckle structure of the far field intensity shows the interference pattern resulting from the apertured near field. The speckles are elongated in the direction perpendicular to the angular orientation of the slit. Power spectra of the far field intensity distribution were studied by taking the 2-D Fourier transform of the far field. The result is shown in Fig. 1c. Because it has the same shape as the near field aperture, the 2-D Fourier transform is a useful tool for determining the slit orientation and aligning the aperture in the near field. More importantly, however, the 2-D Fourier transform is used to evaluate the power spectra. The power spectral density, plotted as a function of wave number in  $\mu\text{m}^{-1}$  in Fig. 1d, is the azimuthal sum of the square of the Fourier amplitudes. This graph indicates the smoothness of the laser beam intensity profile.

## **EXPERIMENTAL SETUP**

The investigation was carried out on the OMEGA Wavefront Sensor (OWS), shown in Fig. 2, and the far field images were recorded on a CCD camera.[1] The alignment was performed with a CW ultraviolet laser. A small fraction of the energy from a pulsed OMEGA laser beam was directed to the OWS and passed through a DPP and an OMEGA lens. It was then down-collimated from a diameter of  $\sim 27.5$  cm to a diameter of 63 mm. A rectangular aperture, shown in Fig. 2, was placed in the near field of the beam with a slit width of 10.5 mm (one-sixth the diameter of the down-collimated beam). The aperture shown in Fig. 3 was mounted on a horizontal translator, and could be rotated to any orientation. Finally, after passing through the aperture the beam was brought to focus on a CCD camera (not shown), where the ultraviolet equivalent-target-plane (UVETP) image was recorded.

## **APERTURE ALIGNMENT**

This investigation required the near field slit to be aligned with each of the two SSD

smoothing axes for separate analysis. In order to measure the angular orientation of the smoothing axes, the measured far field of a laser pulse with 1 THz SSD and no near field aperture was used. The 2-D Fourier transform of a measured far field was calculated for a laser beam smoothed with 1 THz SSD and no near field aperture. This image is shown in Fig. 4. The perpendicular SSD smoothing axes coincide with the 'x' structure seen in Fig. 4. In order to determine the angular orientation of the SSD axes, a computer program was used to rotate the image to a position where one axis appeared horizontal. At this position, a vertical lineout method was used to determine the accuracy of the rotation. The vertical lineout method involved analyzing five vertical columns across the image. These lineouts are plotted in Fig. 5. The image was rotated until the peak values of the five lineouts coincided with the vertical line shown in Fig. 5. Using the vertical lineout method, the orientations of the SSD smoothing axes were determined to be at  $53.5^\circ$  and  $149^\circ$  from the horizontal position of the CCD camera.

Once the angular orientations of the SSD smoothing axes were determined (see Fig. 6a), the aperture on OWS was rotated to these positions. The 2-D Fourier transforms of measured far fields for apertured beams without smoothing were analyzed to check the alignment. Again, the lineout method was used to detect rotation errors, and the slit was adjusted accordingly. Positions of exact angles were noted on the near field aperture, as shown in Fig. 3. 2-D Fourier transforms of far field images produced by this analysis are shown in Fig. 6b and 6c for the two slit orientations.

## **FAR FIELD ANALYSIS**

The near field aperture was accurately aligned along either the smaller or larger SSD bandwidth axes and the far field images for each were recorded. From the measured far fields, 2-D Fourier transforms and power spectra were calculated. Images produced for the smaller SSD bandwidth axis are shown in Fig. 7a and 7b. Images produced for the larger SSD

bandwidth are shown in Fig. 7c and 7d. More smoothing was observed when the slit was aligned with the larger of the SSD bandwidth axis. The normalized power spectra for the two near field slit orientations shown in Fig. 7b (the smaller smoothing axis) and 7d (the larger smoothing axis) are similar for low wave numbers ( $k < 0.4$ ). However, in the higher wave numbers, the power spectral density of the larger SSD bandwidth dropped more sharply. This difference can be seen in Fig. 8c.

## **SIMULATIONS**

The power spectral densities produced by the simulations show good agreement with experimental data, as indicated in Fig. 8a and Fig. 8b. More smoothing was predicted and measured for the slit orientation along the larger SSD bandwidths. However, the amount of smoothing for the larger SSD bandwidth orientation is less than the case with no near field aperture, which is shown in Fig. 9. The  $\sigma_{rms}$  values indicate slight differences between the theoretical and experimental work. These discrepancies will be the subject of further studies.

## **CONCLUSION**

In this study, smoothing by spectral dispersion with apertured near fields was studied. Far field images were recorded and the power spectra of the intensity distributions were analyzed. This investigation shows that the simulations for SSD smoothing of beams with apertured near fields are in good agreement with the experimental results. These results can also be extrapolated to SSD smoothing of beams that irradiate only a portion of the phase plate, such as the ultrafast picket fence pulse.[2]

## **REFERENCES**

- [1] S.P. Regan et al., "Experimental Investigation of Smoothing by Spectral Dispersion", J. Opt. Soc. Am. B **17**, 1483–1489 (2000).
- [2] J.A. Marozas, private communication.

## FIGURE CAPTIONS

### Figure 1

Simulated UVETP images are shown. Near field intensity (the square of the electric field) is shown at (a), indicating constant intensity of an apertured beam. Far field is 2-D Fourier transform of electric field, shown at (b). 2-D Fourier transform of far field at (c) is used to check near field aperture alignment and evaluate power spectra. Power spectral density at (d) is the azimuthal sum of square of the Fourier amplitudes. Normalized power spectral density is plotted as a function of wave number in  $\mu\text{m}^{-1}$  on a logarithmic scale.

### Figure 2

I am adjusting near field aperture on OWS in target bay. Small amount of energy from a pulsed OMEGA laser beam is passed through a DPP and OMEGA lens, and then down-collimated to one-sixth its diameter. Next, it is passed through a rectangular aperture and brought to focus on a CCD camera (not shown), where far fields are measured.

### Figure 3

Near field aperture shown centered on beam on OWS. Aperture placed on horizontal translators and rotated to appropriate position. Marks along outer frame indicate various slit orientations used during experiment.

### Figure 4

2-D Fourier transform of measured far field (shot number 19930) with 1 THz SSD smoothing and no near field aperture. Aperture is aligned with the two SSD axes traced by the concentrated red speckles ('x' pattern).

### Figure 5

Vertical lineouts of 2-D Fourier transform of far field image with 1 THz SSD and no near field aperture shown. Computer program calculates 2-D Fourier transform of far field and rotates

calculated image to angle of  $53.5^\circ$ . Lineouts are taken at five evenly-spaced vertical locations, normalized to peak value, and plotted together. The peaks are offset slightly for viewing ease. The vertical line at 352 on the plot indicates the middle pixel of the image where peaks are expected to fall.

#### Figure 6

SSD axes deduced from lineout method drawn over 2-D Fourier transforms of far field images. Image (a) shows Fig. 4 with SSD axes calculated using lineout shown in Fig. 5. Images (b) and (c) show 2-D Fourier transforms of far fields where near field aperture was aligned along the larger and smaller SSD bandwidths, respectively. The larger SSD bandwidth axis is plotted in (b) and the smaller one is plotted in (c).

#### Figure 7

2-D Fourier transforms and normalized power spectra of far field images of apertured beams smoothed with 1 THz SSD and DPRs are shown. Results with slit aligned along smaller SSD bandwidth axis are shown in (a) and (b) and results with the slit aligned along the larger SSD bandwidth axis are shown in (c) and (d). The power spectra for the slit aligned along the smaller SSD bandwidth axis (b) shows less smoothing than the case with the slit aligned along the larger SSD bandwidth axis (d).

#### Figure 8

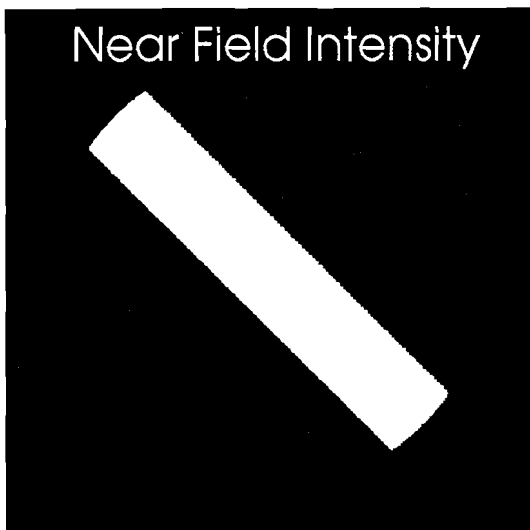
Normalized power spectral density plots indicate that simulations show good agreement with experimental values. In (a), simulation (dotted line) is plotted over experimental results for the slit aligned along the larger SSD bandwidth axis (solid red line). In (b), simulation is plotted over experimental results for the slit aligned along the smaller SSD bandwidth axis (solid green line).

## Figure 9

A comparison of measured power spectra with a near field aperture (solid curve) and without a near field aperture (dotted curve). The near field aperture is aligned along the larger SSD bandwidth axis. In both cases the laser beams are smoothed with 1 THz SSD and distributed polarization rotators. More smoothing is observed without the near field aperture.

Fig. 1

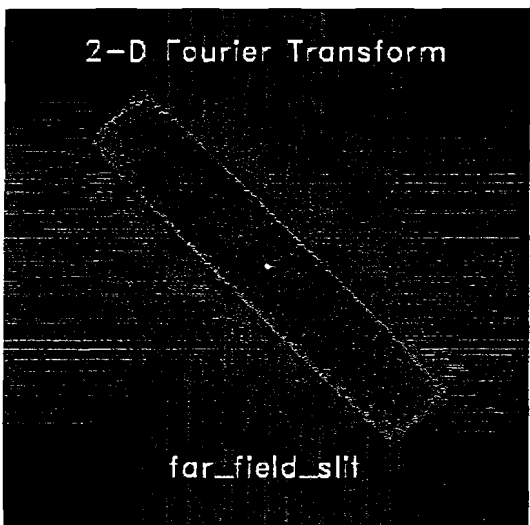
(a)



(b)



(c)



(d)

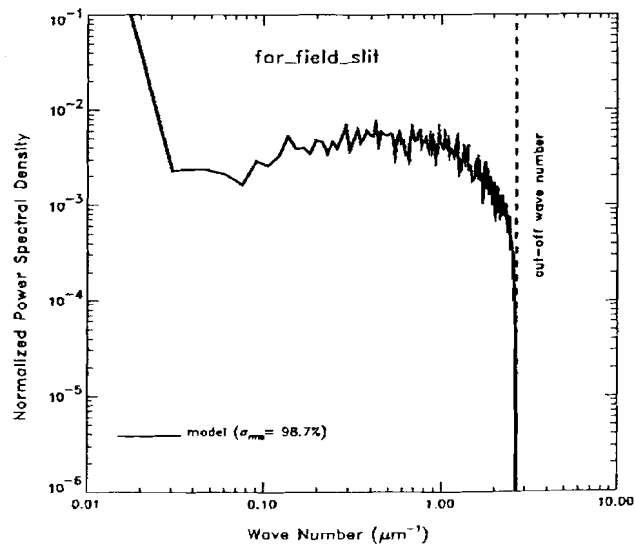


Fig. 2

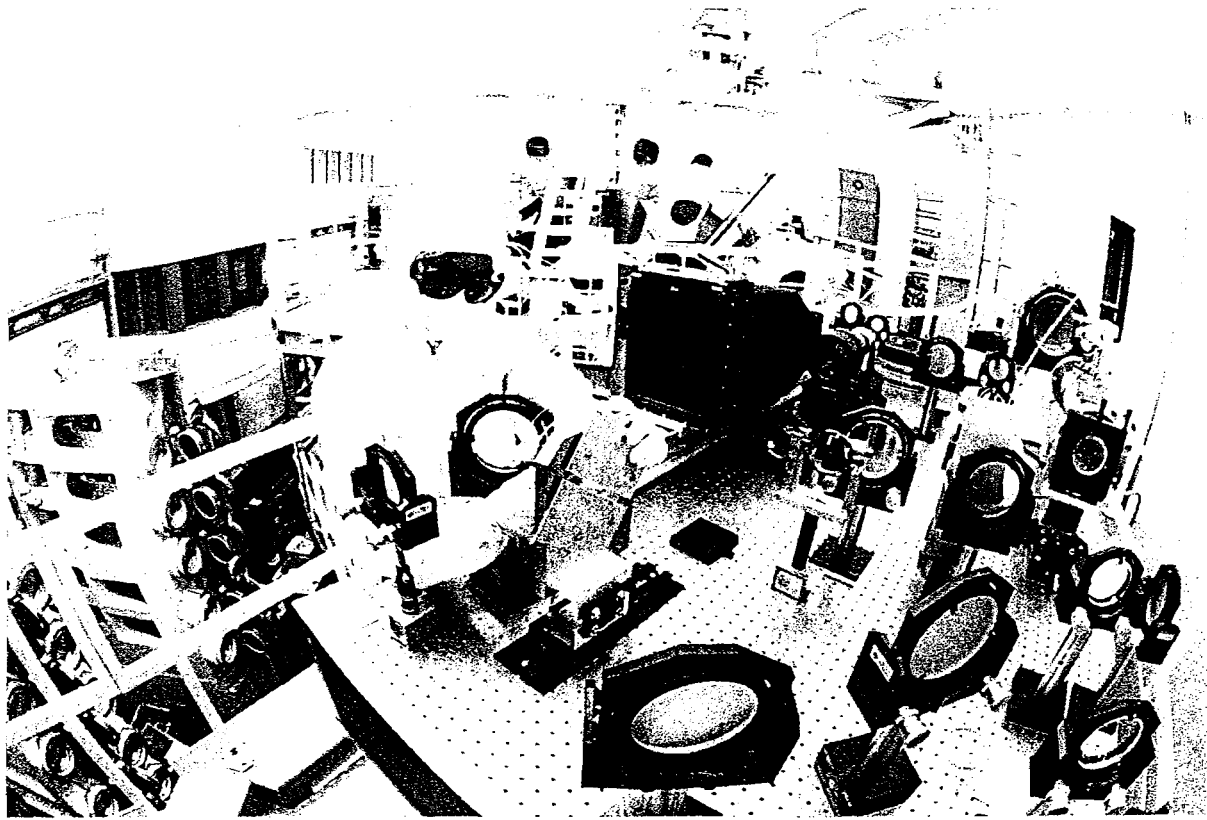


Fig. 3

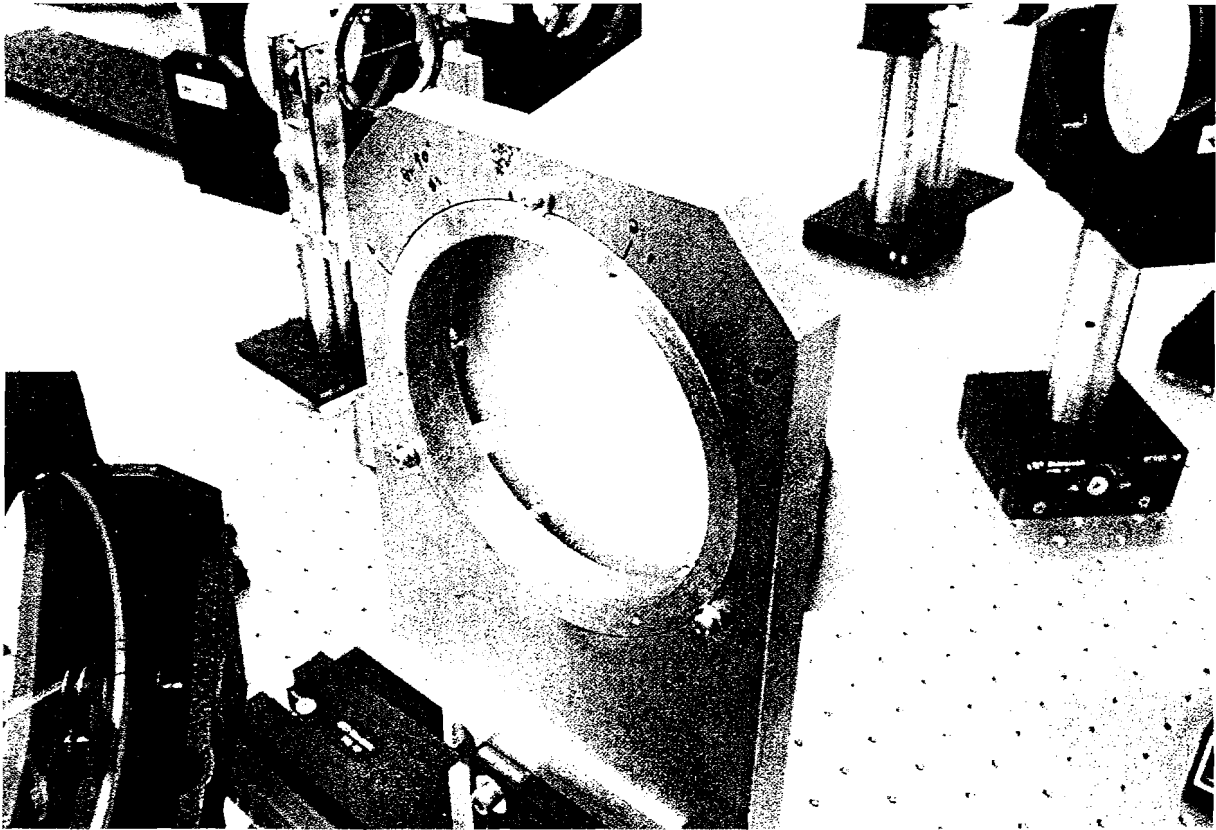


Fig. 4



Fig. 5

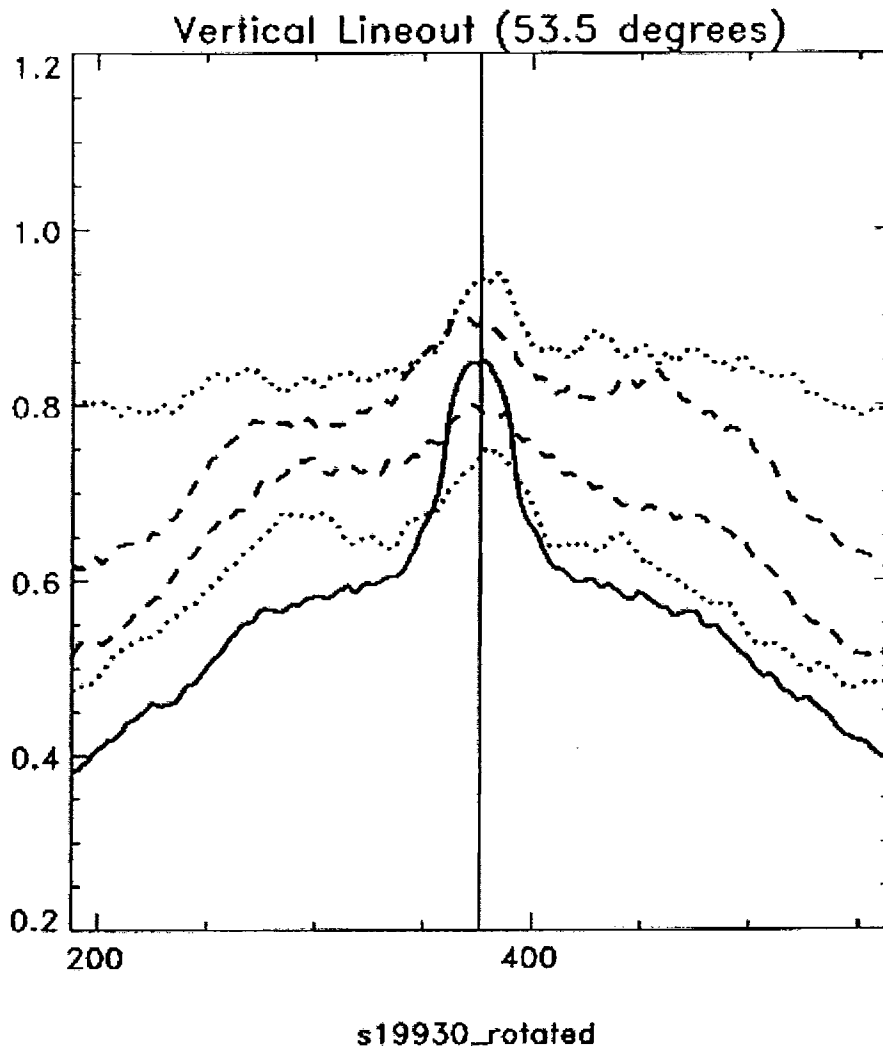
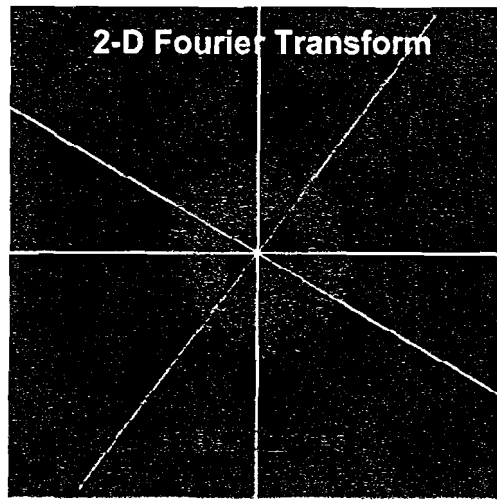
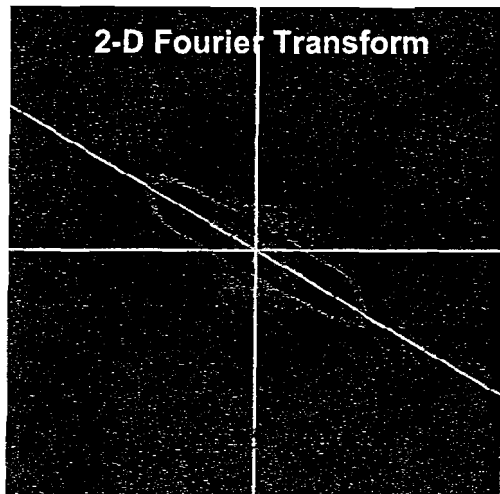


Fig. 6

1 THz SSD  
(a) (no NF aperture)



NF slit aligned to larger  
SSD bandwidth axis  
(b) (no SSD)



NF slit aligned to smaller  
SSD bandwidth axis  
(c) (no SSD)

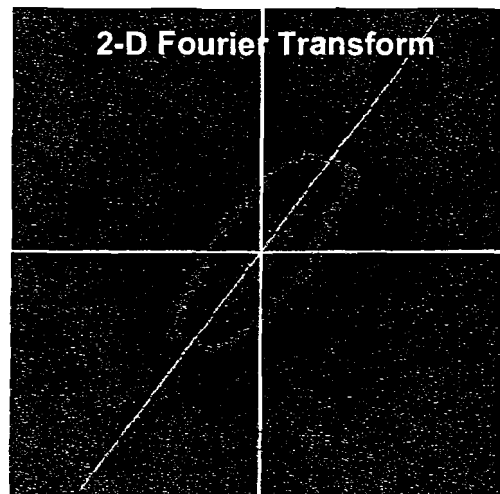


Fig. 7

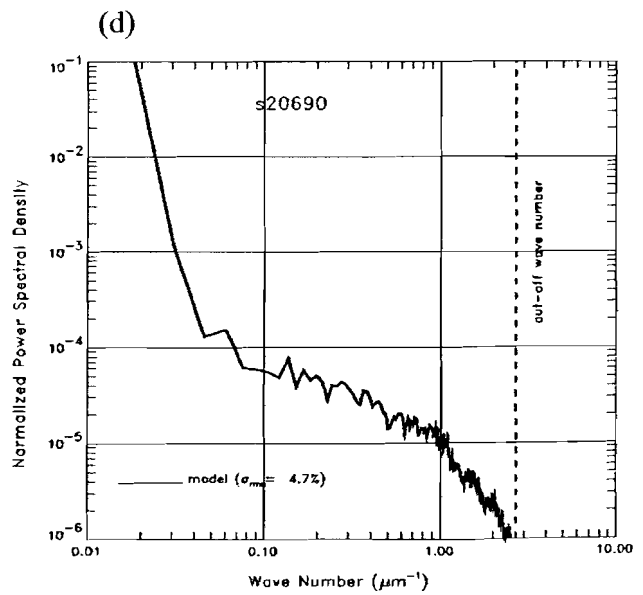
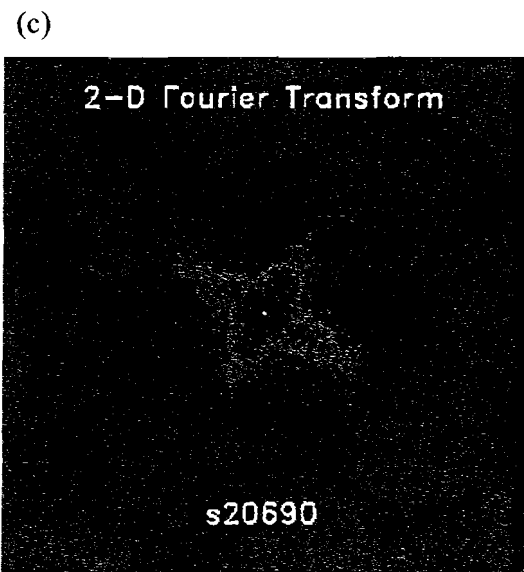
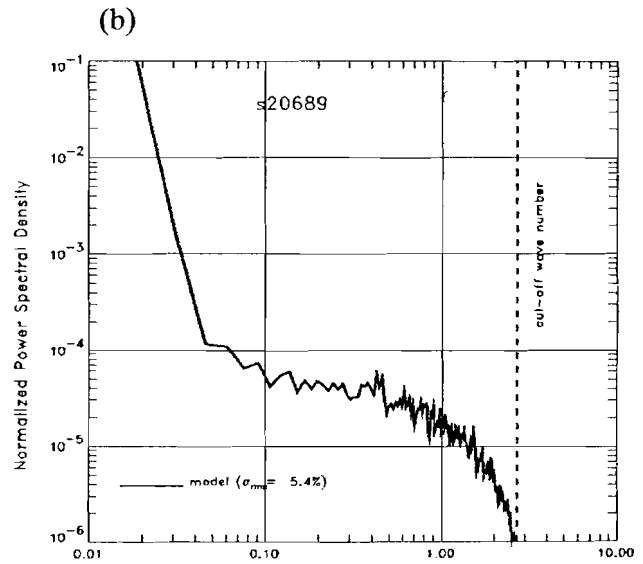
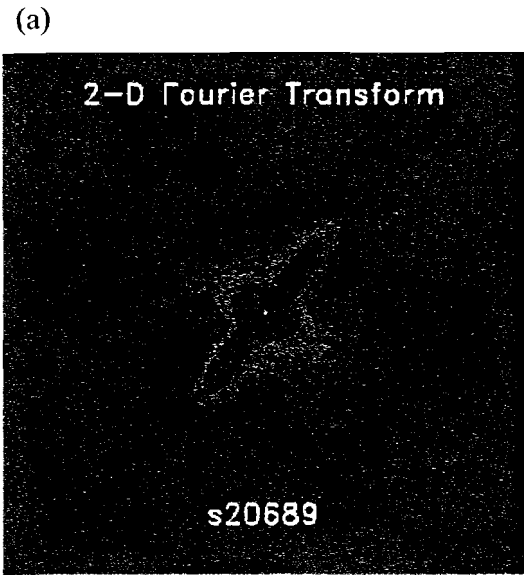


Fig. 8

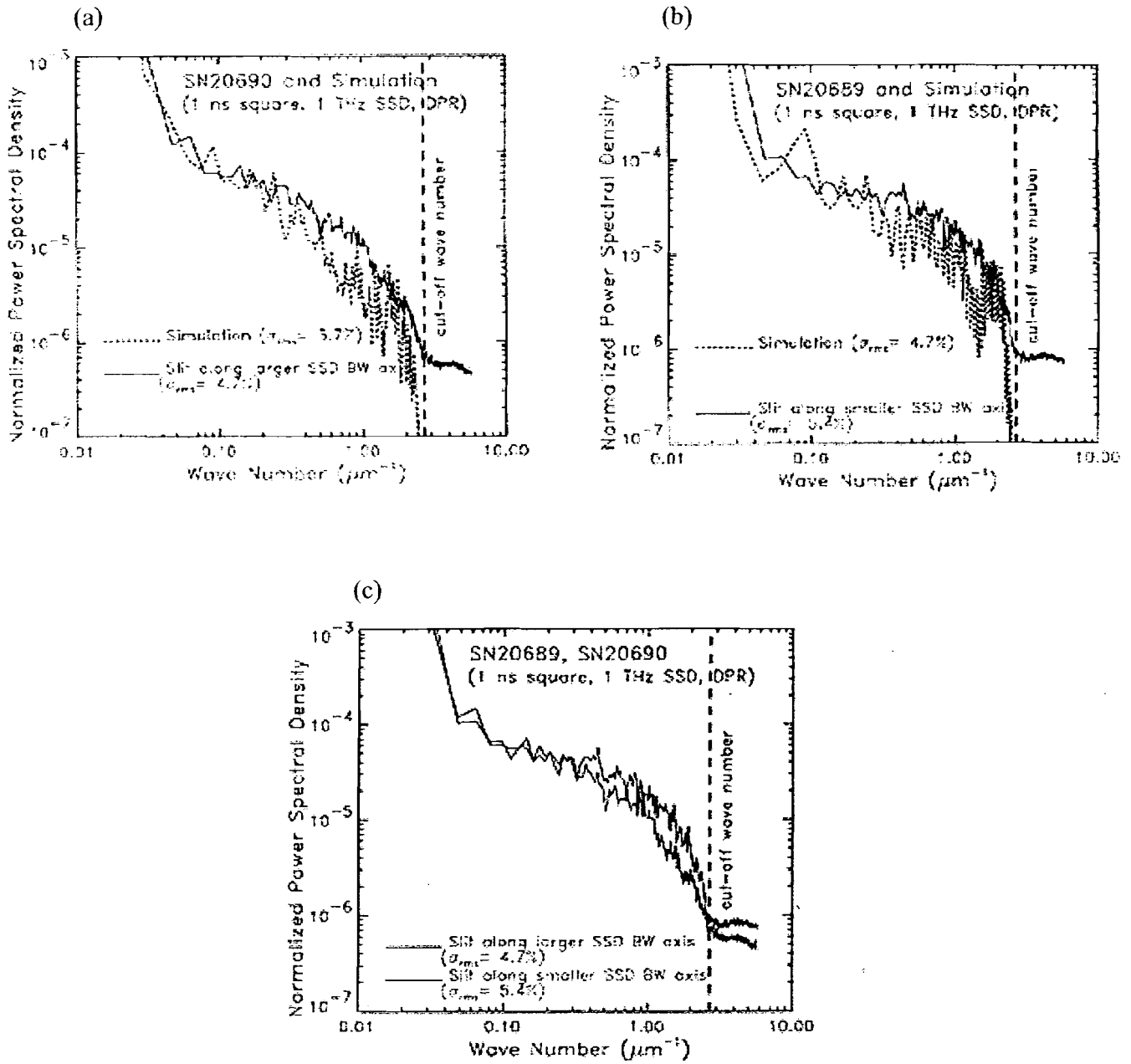


Fig. 9

